ARI The Bulletin of the Istanbul Technical University VOLUME 53, NUMBER 1
Communicated by Metin Gürgöze

Free Vibration Analysis of Circular, Annular and Annular Sectoral Plates

Nihal Eratlı
Department of Civil Engineering, Istanbul Technical University, 34469 Maslak, Istanbul, Turkey
(Received 14 October 2002)

In this study, free vibration analysis of circular, annular and annular sectoral thick plates is carried out by mixed finite element method based on the Gâteaux differential. In free vibration analysis, the problem reduces to the solution of a standard eigenvalue problem and the mixed element is based upon a consistent mass matrix formulation. Bending and torsional moments, transverse shear forces, rotations and displacements are the basic unknowns of the functional. Two different sectoral elements are used with 3×8 degrees of freedom (SEC24) and 4×8 degrees of freedom (SEC32). The accuracy of the SEC24 and SEC32 elements together is verified by applying the method to some problems taken from the literature.

Keywords: Sectoral element, circular plate, annular sectoral plate, finite element, free vibration.

1. Introduction

Plates are used extensively in engineering structures. Therefore extensive researches exist in literature. Several plate theories can be cited like Classical, Reissner and Mindlin. These theories depend greatly on the thickness of the plate. In the classical plate theory which is also called Kirchhoff (thin) plate theory, the influence of transverse shearing strains is neglected. In order to obtain a reliable representation of structural behavior of plates, the refined theories like Reissner and Mindlin have been developed. With the assumption of a linear bending stress distribution and a parabolic shear stress distribution through the thickness of the plate, the Reissner plate theory is derived from the variational principle of the complementary energy [1,2]. By assuming a linear variation of the in-plane displacements across the plate thickness, Mindlin plate theory is obtained from the variational principle of the complementary energy [3]. Depending on Reissner plate theory, the displacement variation is not necessarily linear across the plate thickness and also the deformation of the plate thickness. Reissner and Mindlin theories, can be used to study free vibration of thick plates as well as thin plates. A considerable number of publications are concerned with the problem of the free vibration of circular, annular and annular sectoral plates. [4] based on Mindlin theory, which require C^0 continuity has developed a very efficient form of the bilinear four-node element (S1). [5] have performed free vibration analysis with this element. C^0 continuity causes a problem called shear locking when the plate thickness approaches zero. Various modifications of formulation have been introduced in order to overcome this problem such as reduced / selective integration [6] and Discrete Kirchhoff-Mindlin element [7]. [8] suggests a method to remove zero-energy (kinematics) mode by perturbing the stiffness by stabilization matrix. Recently [9] and [10] have obtained an element for thick plates based on the Reissner theory using the Gâteaux approach, which eliminates shear locking.

In this study, free vibration analysis of circular, annular and annular sectoral Reissner plates is carried out by mixed finite element method using a functional which is based on the Gâteaux differential. The finite elements of various shapes have found application, among the most popular are the rectangular, quadrilateral and triangular elements. For problems involving curved boundaries, the triangular, quadrilateral or curved elements such as sectoral elements may be more suitable. [10] developed two different sectoral elements with 3×8 degrees of freedom (SEC24) and 4×8 degrees of freedom (SEC32). These sectoral elements are ideally suited for the dynamic analysis of circular, annular and annular sectoral plates. In dynamic analysis, the problem reduces to the solution of a standard eigenvalue problem and the mixed element is based upon a consistent mass matrix formulation. The accuracy of the present method is discussed for circular plates with different edge conditions, annular and annular sectoral plates, and compared to the results calculated by the other methods.

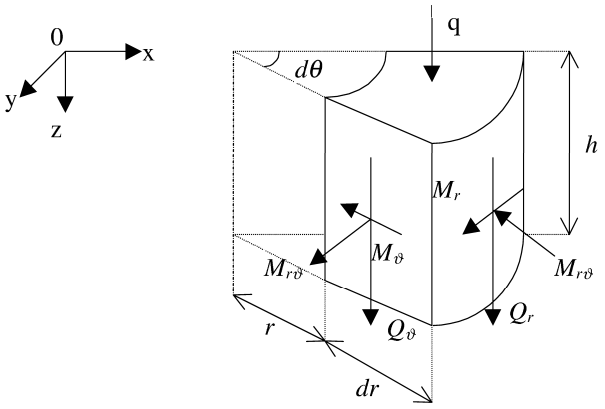

Figure 1. The positive directions of internal forces

2. The field equations of thick plate in polar coordinates

Reissner plate theory includes the transverse shear effects and field equations of a plate element h r dr dθ (Fig. 1) in polar coordinates are given in Eq. (1) [10,11].

$$\frac{\partial M_r}{\partial r}+\frac{1}{r}\frac{\partial M_{\theta r}}{\partial \theta}+\frac{M_r-M_\theta}{r}-Q_r=0, \quad (1.a)$$

$$\frac{\partial M_{r\theta}}{\partial r}+\frac{1}{r}\frac{\partial M_\theta}{\partial \theta}+\frac{2M_{r\theta}}{r}-Q_\theta=0, \quad (1.b)$$

$$\frac{\partial Q_r}{\partial r}+\frac{1}{r}\frac{\partial Q_\theta}{\partial \theta}+\frac{Q_r}{r}+q=0, \quad (1.c)$$

$$\Omega_\theta+\frac{1}{r}\frac{\partial \mathrm{w}}{\partial \theta}-\frac{6}{5Gh}Q_\theta=0, \quad (1.d)$$

$$\frac{\partial \Omega_r}{\partial r}-\frac{12}{Eh^3}[M_r-\nu M_\theta]=0, \quad (1.e)$$

$$\frac{1}{r}\frac{\partial \Omega_\theta}{\partial \theta}+\frac{\Omega_r}{r}-\frac{12}{Eh^3}[M_\theta-\nu M_r]=0, \quad (1.f)$$

$$\frac{\partial \Omega_\theta}{\partial r}+\frac{1}{r}\frac{\Omega_r}{\partial \theta}-\frac{\Omega_\theta}{r}-\frac{12}{Eh^3}M_{r\theta}=0. \quad (1.g)$$

In symbolic form, dynamic (natural) boundary conditions can be written as,

$$\begin{aligned}&\mathbf{M}-\hat{\mathbf{M}}=\mathbf{0},\\ &\mathbf{Q}-\hat{\mathbf{Q}}=\mathbf{0},\end{aligned} \quad (2)$$

and geometric (kinematic) boundary conditions are

$$\begin{aligned}&\mathbf{w}-\hat{\mathbf{w}}=\mathbf{0},\\ &\mathbf{\Omega}-\hat{\mathbf{\Omega}}=\mathbf{0}.\end{aligned} \quad (3)$$

The explicit form of the boundary conditions will be obtained after some variational manipulations. In Eq. (2) and Eq. (3) quantities with hat are known values on the boundary. $\mathbf{M}$, $\mathbf{Q}$, Ω , $\mathbf{w}$ are the moment, force, rotation and deflection vectors, respectively. Field equations for Reissner plate in polar coordinates can be written in operator form as,

$$\mathbf{Q}=\mathbf{L}\mathbf{y}-\mathbf{f}. \quad (4)$$

The matrix form of the operator is given in [10] in detail.

3. Functional for thick plates in polar coordinates

If the operator $\mathbf{Q}$ in Eq. (4) is potential, the equality

$$< d\mathbf{Q}(\mathbf{y},\bar{\mathbf{y}}),\mathbf{y}^\star >=< d\mathbf{Q}(\mathbf{y},\mathbf{y}^\star),\bar{\mathbf{y}} > \quad (5)$$

must be satisfied [12]. $d\mathbf{Q}(\mathbf{y},\bar{\mathbf{y}})$ and $d\mathbf{Q}(\mathbf{y},\mathbf{y}^\star)$ are Gâteaux derivatives of the operator in directions of $\bar{\mathbf{y}}$ and $\mathbf{y}^\star$ which are constant elements in the domain. Gâteaux derivative of the operator is defined as;

$$d\mathbf{Q}(\mathbf{u},\bar{\mathbf{u}})=\left.\frac{\partial Q(\mathbf{u}+\tau\bar{\mathbf{u}})}{\partial \tau}\right|_{\tau=0} \quad (6)$$

where τ is a scalar. Using this definition, after some simple manipulations it can be shown that Eq. (5) holds and the operator $\mathbf{Q}$ is a potential operator. To satisfy this equality the explicit forms of the boundary conditions must be as follows;

$$\begin{aligned}&[M,\Omega]=[\Omega_r,(M_r+\frac{1}{r}M_{r\theta})]+[\Omega_\theta,(M_{r\theta}+\frac{1}{r}M_\theta)],\\ &[Q,\mathrm{w}]=[(Q_r+Q_\theta),\mathrm{w}].\end{aligned} \quad (7)$$

Since the operator is potential then the functional corresponding to the field equations is obtained as;

$$\mathbf{I}(\mathbf{y})=\int_0^1[\mathbf{Q}(s\mathbf{y}),\mathbf{y}]\,ds, \quad (8)$$

where s is a scalar quality. Functional $I_p(\mathbf{y})$ can be obtained after some manipulations as;

$$\begin{aligned} I_p &= [Q_r, (\Omega_r + \mathrm{w}_{,r})] + [Q_\theta, (\Omega_\theta + \frac{1}{r}\mathrm{w}_{,\theta})] \quad (9)\\ &+ [M_r, \Omega_{r,r}] + [\frac{1}{r}M_\theta, (\Omega_{\theta,\theta} + \Omega_r)]\\ &+ [M_{r\theta}, (\frac{1}{r}\Omega_{r,\theta} + \Omega_{\theta,r} - \frac{1}{r}\Omega_\theta)]\\ &- \frac{6}{Eh^3}\{[M_r, M_r] + [M_\theta, M_\theta] - 2\nu[M_r, M_\theta]\\ &+ 2(1+\nu)[M_{r\theta}, M_{r\theta}]\} - \frac{3}{5Gh}\{[Q_r, Q_r]\\ &+ [Q_\theta, Q_\theta]\} - [q, \mathrm{w}] - [(\Omega - \hat{\Omega}), M]_\epsilon\\ &- [(\mathrm{w} - \hat{\mathrm{w}}), Q]_\epsilon - [\hat{M}, \Omega]_\sigma - [\hat{Q}, \mathrm{w}]_\sigma. \end{aligned}$$

The braces with the σ index and ϵ index are valid on the boundary where the dynamic boundary conditions and the geometric boundary conditions are prescribed, respectively. Where [,] is the inner product and defined as follows;

$$[f, g] = \int\int f(r,\theta)\, g(r,\theta)\, r\, dr\, d\theta. \quad (10)$$

For the free vibration analysis, the functional given by Eq. (9) is valid only by letting [q,w]=$1/2\,\rho\omega^2$ [w,w] as far as the harmonic solutions are required. If the variational derivative of the functional in Eq. (9) is taken, all the field equations and boundary conditions can be reproduced.

The same functional can be obtained by the Hellinger-Reissner principle, but it is believed that the Gâteaux approach has the following advantages over the Hellinger-Reissner approach:

1. The field equation must be consistent [13]. Gâteaux differential method provides consistency of field equations [14].
2. During the potential test, boundary conditions can be constructed.
3. All the field equations are enforced to the functional in a systematic manner.

Let w be the displacement in z-direction, $[\Omega_r]$ and $[\Omega_\theta]$ being the rotations of the cross-sections normal to in rz and θz planes. Q_r, Q_θ are shear forces and $M_r, M_\theta, M_{r\theta}$ are the bending and torsional moments in polar coordinates. They are nodal unknowns of the generated finite element and expressed by shape functions (ψ_i) which are given in Appendix II. For example, w(r,θ,t)=sin ωt $\Sigma \mathrm{w}_i\psi_i(s,\eta)$ where w_i are the

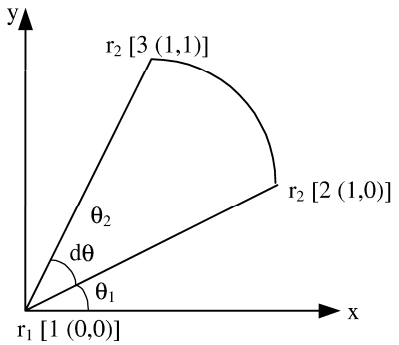

Figure 2. SEC24 element

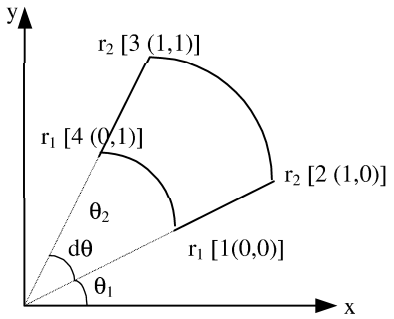

Figure 3. SEC32 element

nodal values and i=1,...,n (n=number of nodes of the element). In the finite element formulation of thick plates, two different elements which is depicted in (Fig. 2) and (Fig.3) are used. One of these elements is SEC24 which has an element with 24 degrees of freedom, and with 8 degrees of freedom per node. The other one is SEC32 which has 32 degrees of freedom element with 8 degrees of freedom per node. The finite element matrices $[k]_{24}$, $[k]_{32}$ for SEC24 and SEC32 are obtained by variational principles from Eq. (9). These element matrices and the explicit form of the submatrices of these elements ($[K_1]_{24}$, $[K_2]_{24}$, $[K_3]_{24}$, $[K_4]_{24}$, $[K_1]_{32}$, $[K_2]_{32}$, $[K_3]_{32}$, $[K_4]_{32}$) are given in Appendix II.

4. Free vibration analyze

The problem of determining the natural vibration frequencies of a structural system reduces to

the solution of a standard eigenvalue problem,

$$[\mathbf{K}] - \omega^2 [\mathbf{M}] = 0, \tag{11}$$

where $[\mathbf{K}]$ is the system matrix, $[\mathbf{M}]$ is the mass matrix for the entire domain and ω is the natural angular frequency of the system. The explicit form of Eq. (11) is

$$\left(\begin{bmatrix} [\mathbf{K_{11}}] & [\mathbf{K_{12}}] \\ [\mathbf{K_{12}}]^T & [\mathbf{K_{22}}] \end{bmatrix} - \omega^2 \begin{bmatrix} 0 & 0 \\ 0 & [\mathbf{M}] \end{bmatrix} \right) \times \begin{Bmatrix} \{\mathbf{F}\} \\ \{\mathbf{w}\} \end{Bmatrix} = \begin{Bmatrix} \{0\} \\ \{0\} \end{Bmatrix}, \tag{12}$$

where $\{\mathbf{F}\} = \{\mathbf{M}\,\mathbf{Q}\,\mathbf{\Omega}\}^T, \{\mathbf{w}\}$ are moments, shear forces, rotations and displacement vectors, respectively. Elimination of $\{\mathbf{F}\}$ from Eq. (12) gives

$$([\mathbf{K}^*] - \omega^2 [\mathbf{M}]) \{\mathbf{w}\} = \{0\}, \tag{13}$$

where

$$[\mathbf{K}^*] = [\mathbf{K_{22}}] - [\mathbf{K_{12}}]^T [\mathbf{K_{11}}]^{-1} [\mathbf{K_{12}}], \tag{14}$$

and $[\mathbf{K}^*]$ is the condensed system matrix of the problem. If there is no foundation, then $[\mathbf{K_{22}}] = 0$. The element mass matrix is based upon consistent mass formulation as,

$$[m] = \rho\, h\, [K_1]. \tag{15}$$

where h is the plate thickness, ρ is the mass density and $[K_1]$ is given in Appendix II.

5. Numerical examples

Free vibration of circular plates has been investigated intensively in the literature. In order to check the applicability and accuracy of the proposed mixed finite element formulation of thick sectoral plates, various problems are solved and results are compared with some existing studies in the literature. Example problems will display the properties of the SEC24-SEC32 elements for plate vibration.

Example 1. The simply supported circular plate and shear locking test for dynamic analysis

In the present example, a simply supported circular plate is considered and frequency parameters are obtained for different meshes. The convergence of frequency parameters is sketched in Fig. (4). Values of frequency parameter ($\bar{\omega} = \omega\, a^2 \sqrt{\bar{\rho}/D}$) found using SEC24-SEC32 are tabulated in Table 1, where n, s refers to the number of radial and circumferential nodes, respectively. 288 elements are used in calculation. 8 and 36 elements exist in radial and angular directions, respectively. Inspection of Table 1 shows that, the frequency parameters obtained by Reissner plate theory are lower than the ones given by [15] as expected. The plate thickness affects the behavior of the plate. It is well known that, the shear deformation becomes important as the ratio of plate thickness to the radius of plate (h/a) decreases. The comparison of first frequency parameter ($\bar{\omega}_{00}$) variations for simply supported circular plate and for different plate thicknesses is given in Fig. (5). It can be seen that Kirchhoff plate theory is valid for the value of a/h higher than 20. Similar comparisons can be also given for higher frequency parameters in Fig. (6). It is observed that this ratio increase with the increasing frequency parameters, e.i. a/h reaches to 50 for $\bar{\omega}_{10}$, $\bar{\omega}_{20}$, $\bar{\omega}_{01}$, $\bar{\omega}_{30}$. On the other hand, Reissner plate theory is valid for analysis thick as well as thin plates. Shear locking effects are tested as far as a/h=10^4 and it is observed that sectoral elements are free from shear locking. Fig. (7) shows mesh which is used in calculation. The contour lines of $\bar{\omega}_{00}$, $\bar{\omega}_{10}$, $\bar{\omega}_{20}$ are shown in Fig. (8).

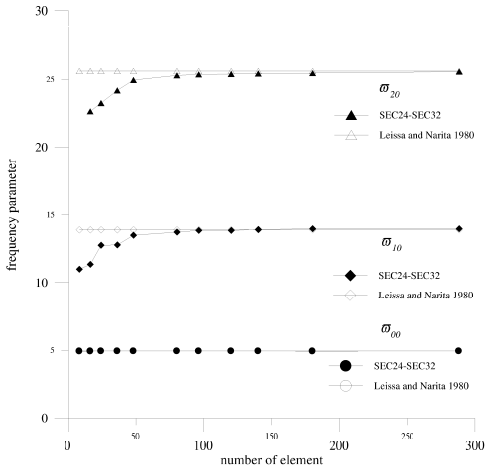

Figure 4. Convergence of frequence parameters in simply supported circular plate for different meshes

Table 1
Frequency parameters ($\bar{\omega} = \omega\, a^2 \sqrt{\bar{\rho}/D}$) for simply supported circular plate (ν=0.3)

	n=0	n=1	n=2	n=3	n=4	n=5	n=6	n=7	n=8	n=9	n=10
s=0	4.93	13.98	25.56	39.94	56.73	75.81	96.86	119.92	145.79	175.69	208.45
	(4.93)	(13.89)	(25.61)	(39.95)	(56.84)	(76.20)	(97.99)	(122.17)	(148.72)	(177.61)	(208.81)
s=1	29.68	47.79	69.41	93.58	119.04	148.29	178.15	213.22	247.09	285.01	
	(29.72)	(48.47)	(70.11)	(94.54)	(121.70)	(151.51)	(183.94)	(218.95)	(256.49)	(296.54)	
s=2	73.27	97.76	132.51	167.24	205.51	244.30	281.22	326.17	373.82		
	(74.15)	(102.77)	(134.29)	(168.67)	(205.85)	(245.77)	(288.41)	(333.72)	(381.66)		
s=3	137.01	175.69	212.30	259.55	305.78	357.22	406.63	458.18			
	(138.31)	(176.80)	(218.20)	(262.48)	(309.60)	(359.53)	(412.22)	(467.64)			
s=4	213.02	266.64	306.83	373.82	406.06	485.97	550.32				
	(222.21)	(270.56)	(321.84)	(376.01)	(433.04)	(492.91)	(555.59)				
s=5	312.24	379.61	431.24	489.04							
	(325.84)	(384.06)	(445.21)	(509.26)							
s=6	406.64	503.13									
	(449.22)	(517.3)									

(...) are taken from Leissa 1969 [16].

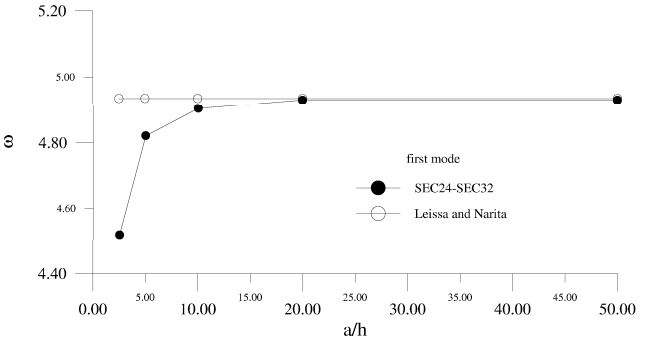

Figure 5. Shear locking test for first frequency parameter

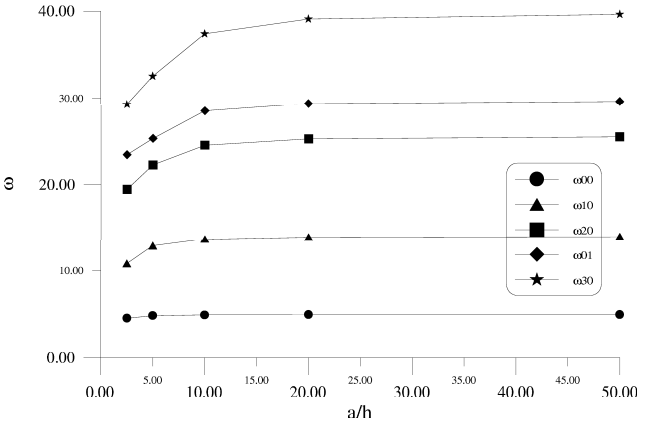

Figure 6. Shear locking test for several frequency parameters

Example 2. Circular plate clamped all around

The frequency parameters of clamped circular plate are obtained by using SEC24-SEC32 and compared with [16]. Values of frequency parameter ($\bar{\omega} = \omega\, a^2 \sqrt{\bar{\rho}/D}$) obtained using SEC24-SEC32 are tabulated in Table 2, where n, s refers to the number of radial and circumferential nodes, respectively. The total number of elements used in calculation are 288. 8 and 36 elements exist in radial and angular directions, respectively. The frequency parameters obtained by Reissner plate theory are lower than the ones given by Kirchhoff plate theory.

Example 3. Completely free circular plate

The frequency parameters ($\bar{\omega} = \omega\, a^2 \sqrt{\bar{\rho}/D}$) of the completely free plate obtained using SEC24-SEC32 are tabulated in Table 3, where n, s refers to the number of radial and circumferential nodes, respectively and compared with [16]. The total number of elements used in calculation are 288. 8 and 36 elements exist in radial and angular directions, respectively. The frequency parameters obtained by Reissner plate theory are lower than the ones given by Kirchhoff

Table 2
Frequency parameters ($\bar{\omega} = \omega\, a^2 \sqrt{\bar{\rho}/D}$) for clamped circular plate (ν=0.3)

	n=0	n=1	n=2	n=3	n=4	n=5	n=6	n=7	n=8	n=9	n=10
s=0	10.21	21.19	34.63	50.73	69.06	89.57	111.96	135.50	161.29	194.76	230.69
	(10.21)	(21.26)	(34.88)	(51.04)	(69.66)	(90.73)	(114.21)	(140.05)	(168.24)	(198.75)	(231.57)
s=1	39.50	59.06	83.59	109.38	135.57	169.90	204.67	233.12	269.84	297.46	359.07
	(39.77)	(60.82)	(84.58)	(111.01)	(140.10)	(171.80)	(206.07)	(242.87)	(282.19)	(324.00)	(368.27)
s=2	85.96	111.96	150.95	190.11	226.05	269.84	310.74	359.07			
	(89.10)	(120.08)	(153.81)	(190.30)	(229.51)	(271.42)	(316.00)	(363.20)			
s=3	156.01	194.76	233.12	286.58	331.49	385.35					
	(158.18)	(199.06)	(242.71)	(289.17)	(338.41)	(390.38)					
s=4	244.13	297.46	339.70	407.66							
	(247.00)	(297.77)	(351.38)	(407.72)							
s=5	354.14										
	(355.56)										

(...) are taken from Leissa 1969 [16].

Table 3
Frequency parameters ($\bar{\omega} = \omega\, a^2 \sqrt{\bar{\rho}/D}$) for completely free circular plate (ν=0.33)

	n=0	n=1	n=2	n=3	n=4	n=5	n=6
s=0	...	...	5.24	12.19	21.36	32.63	45.81
			(5.353)	(12.23)	(21.60)	(33.10)	(46.20)
s=1	9.06	20.48	35.13	51.69	72.40	94.83	120.8
	(9.08)	(20.52)	(35.25)	(52.91)	(73.10)	(95.80)	(121.0)
s=2	36.68	58.86	83.31	110.5	138.06	173.8	207.3
	(38.55)	(59.86)	(83.90)	(111.3)	(142.8)	(175.0)	(210.3)
s=3	85.99	116.6	152.6	190.6	230.4	274.5	312.4
	(87.80)	(119.0)	(154.0)	(192.1)	(232.3)	(274.6)	(319.7)
s=4	153.8	192.8	238.8	279.9	338.7	390.5	430.4
	(157.0)	(198.2)	(242.7)	(290.7)	(340.4)	(392.4)	(447.3)
s=5	240.8	296.7	349.2	405.6	456.7	526.4	549.1
	(245.9)	(296.9)	(350.8)	(408.4)	(467.9)	(529.5)	(593.9)

(...) are taken from Leissa 1969 [16].

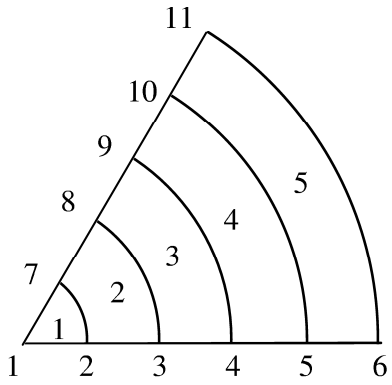

Figure 7. Typical circular plate mesh with 5 element

plate theory.

Example 4. The annular plate

In the literature, a considerable amount of work has been reported on the vibration of thin annular plates. It is well known that, the effect of shear deformation, cause decreases in the computed frequency parameters ($\bar{\omega} = \omega a^2 \sqrt{\bar{\rho}/D}$), just like circular plates. Free-simply supported annular plate shown in Fig. (9) is analyzed and the frequency parameters of the annular plate obtained using SEC32 are tabulated in Table 4 for various values of (b/a) versus a/h, where n, s refers to the number of radial and circumferential nodes, respectively. The total number of elements used in calculation are 288. 8 and 36 elements exist in radial and angular directions, respectively. It can be observed that, the frequency parameters obtained by Reissner plate theory (SEC32) and Kirchhoff plate theory [16] decrease with a decreasing in the thickness ratio (a/h) and the radii ratio (b/a). The frequency parameters obtained by Reissner plate theory are lower than the ones given by Kirchhoff plate theory. [17,18] have used thick plate theories and obtained the same trend as present theory (SEC32) when plate thickness was changed. The contour line of $\bar{\omega}_{00}$ is shown in Fig. (10).

Example 5. Annular sectoral plates

Annular sectoral plates with two different boundary conditions (all sides simply supported

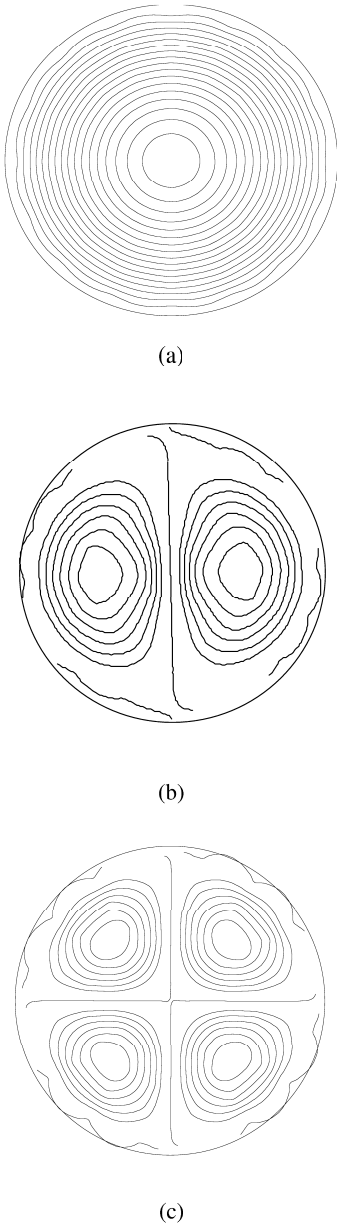

Figure 8. a. The counter line of ω_{00} for simply supported circular plate. b. The counter line of ω_{10} for simply supported circular plate c. The counter line of ω_{20} for simply supported circular plate

Table 4
Frequency parameters ($\bar{\omega} = \omega\, a^2 \sqrt{\bar{\rho}/D}$) for free-simply supported annular plates (ν=0.3)

		b/a=0.00005			b/a=0.1			b/a=0.3			b/a=0.5		
n	s a/h	5	10	50	5	10	50	5	10	50	5	10	50
0	1	4.78	4.87	4.90	4.70	4.77	4.80	4.57	4.63	4.64	5.00	5.05	5.06
				(4.97)			(4.86)			(4.66)			(5.07)
	2	25.53	28.28	29.37	25.82	28.42	29.43	31.05	35.60	37.35	51.73	62.08	66.45
				(29.76)			(29.40)			(37.00)			(65.80)
1	1	12.81	13.56	13.84	12.54	13.31	13.62	11.73	11.96	12.33	9.98	10.71	11.04
				(13.94)			(13.90)			(12.80)			(11.60)
	2	37.16	43.68	46.60	37.66	44.29	47.32	36.48	41.79	43.98	53.13	62.33	67.86
				(48.51)			(48.00)			(45.80)			(69.90)
2	1	22.25	24.52	25.46	22.02	24.24	25.17	20.71	22.99	23.71	18.55	20.51	21.44
				(25.65)			(25.40)			(24.10)			(22.30)
	2	53.12	64.92	68.57	47.09	63.50	65.82	43.13	57.57	62.20	58.63	72.01	78.54
				(70.14)			(69.20)			(65.10)			(81.10)

(...) are taken from Leissa 1969 [16].

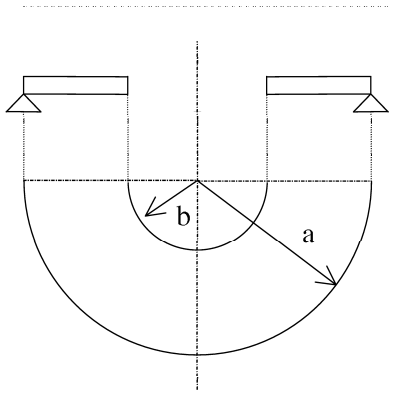

Figure 9. The annular plate

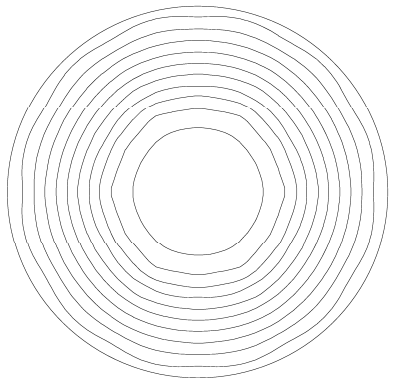

Figure 10. The counter line of ω_{00} for annular plate

and clamped) (Fig. 11) are considered for various thickness ratios. Therefore, two examples are analyzed by using SEC32. 192 elements are used in calculation. 12 and 16 elements exist in radial and angular directions, respectively.

In the first example, the annular sectoral plate like fan shape (b/a=0.00001) and sectoral shape (b/a=0.4) with all edges simply supported are solved. The results obtained for two types are tabulated in Tables 5-6. As a second example, the plate, which has same geometry, is solved for clamped edges and the results are given in Tables 7-8. The contour lines of frequency parameters for sectoral plate with simply supported are given in Fig. (12).

The present results are in a good agreement with the other studies using different methods [19,22]. It is seen that the frequency parameters are found to decrease with increasing sectoral angles (α) and increasing thickness. The effects of different boundary conditions can also be observed. By comparing simply supported and clamped boundary conditions, The frequency parameters for the simply supported sectoral plates much lower than the clamped sectoral plates. These results show that the frequency parameters increase with increasing rigidity of plates.

Example 6. Circular plates on an elastic foundation

In order to demonstrate the efficiency of SEC24 and SEC32 elements, the free vibration analyze

Table 5
Frequency parameters ($\bar{\omega} = \omega\, a^2 \sqrt{\bar{\rho}/D}$) for fan shape sectorial plates with simply supported boundary conditions (ν=0.3),(b/a=0.00001)

α	h/a	1	2	3	4	5	6
$\pi/6$	0.001	97.93	183.22	278.05	283.95	393.27	427.10
$\pi/6$	0.1	83.55	143.86	203.15	205.53	264.15	281.41
$\pi/6$	0.2	64.80	101.56	134.00	135.46	174.28	178.89
$\pi/4$	0.001	56.722	121.40	148.71	203.82	255.17	277.85
$\pi/4$	0.1	51.07	101.86	121.74	158.47	190.47	203.92
$\pi/4$	0.2	42.45	76.55	88.59	109.83	127.23	134.32
$\pi/3$	0.001	39.87	94.36	97.90	167.67	177.29	183.29
$\pi/3$	0.1	36.80	81.85	84.70	135.06	138.66	145.96
$\pi/3$	0.2	31.76	63.85	65.63	96.53	98.49	100.36
$\pi/2$	0.001	25.76	56.77	70.91	97.93	121.39	135.92
$\pi/2$	0.1	24.14	51.73	62.75	85.06	103.19	111.57
$\pi/2$	0.2	21.66	43.07	51.06	64.73	77.46	82.96

Table 6
Frequency parameters ($\bar{\omega} = \omega\, a^2 \sqrt{\bar{\rho}/D}$) for sectorial plates with simply supported boundary conditions (ν=0.3),(b/a=0.4)

α	h/a	1	2	3	4	5	6
$\pi/6$	0.001	98.74	195.26	277.94	334.46	431.31	521.87
$\pi/6$	0.1	83.421	149.66	202.83	232.22	283.02	325.02
$\pi/6$	0.2	64.73	105.18	133.94	144.28	149.71	175.13
$\pi/4$	0.001	60.32	147.93	148.87	260.24	277.79	285.51
$\pi/4$	0.1	52.77	119.65	121.42	192.12	199.94	203.54
$\pi/4$	0.2	43.62	87.47	88.46	128.26	134.24	136.48
$\pi/3$	0.001	46.13	98.71	131.31	177.31	195.11	268.00
$\pi/3$	0.1	41.215	84.645	109.23	141.60	151.83	199.54
$\pi/3$	0.2	34.966	65.60	81.05	98.41	106.18	131.79
$\pi/2$	0.001	36.10	60.30	98.74	119.72	147.95	148.43
$\pi/2$	0.1	33.06	53.52	85.02	101.93	120.67	122.03
$\pi/2$	0.2	28.68	44.19	65.88	76.56	87.96	88.83

Table 7
Frequency parameters ($\bar{\omega} = \omega\, a^2 \sqrt{\bar{\rho}/D}$) for fan shape sectorial plates with clamped boundary conditions (ν=0.3),(b/a=0.00001)

α	h/a	1	2	3	4	5	6
$\pi/6$	0.001	188.82	295.31	422.05	432.62	529.11	581.62
$\pi/6$	0.1	130.65	187.09	225.67	241.84	296.15	312.43
$\pi/6$	0.2	82.54	113.74	132.07	142.21	172.36	179.93
$\pi/4$	0.001	107.82	189.86	225.42	308.15	346.41	378.90
$\pi/4$	0.1	84.96	136.03	155.59	180.87	219.45	233.12
$\pi/4$	0.2	58.63	88.08	98.67	118.38	133.78	140.77
$\pi/3$	0.001	75.86	144.33	149.38	225.53	243.06	248.44
$\pi/3$	0.1	63.29	110.49	113.38	158.70	167.34	169.19
$\pi/3$	0.2	46.31	74.69	76.31	100.07	104.65	107.97
$\pi/2$	0.001	48.77	87.67	104.60	136.46	164.03	178.59
$\pi/2$	0.1	43.23	73.33	85.39	107.46	125.15	133.92
$\pi/2$	0.2	33.89	53.52	60.90	74.45	84.60	89.59

Table 8
Frequency parameters ($\bar{\omega} = \omega\, a^2 \sqrt{\bar{\rho}/D}$) for sectorial plates with clamped boundary conditions (ν=0.3),(b/a=0.4)

α	h/a	1	2	3	4	5	6
$\pi/6$	0.001	188.16	305.05	418.32	452.09	598.87	658.23
$\pi/6$	0.1	130.08	192.52	241.49	264.88	314.63	349.40
$\pi/6$	0.2	82.82	117.19	142.18	156.17	180.65	200.23
$\pi/4$	0.001	111.22	219.56	224.86	356.05	373.19	376.02
$\pi/4$	0.1	87.46	153.37	155.49	222.79	232.52	234.36
$\pi/4$	0.2	60.44	97.86	98.73	135.51	140.66	142.06
$\pi/3$	0.001	85.24	149.74	194.51	241.95	266.68	357.03
$\pi/3$	0.1	70.078	114.11	139.55	168.97	181.03	223.51
$\pi/3$	0.2	50.49	76.86	90.38	107.95	113.81	136.62
$\pi/2$	0.001	69.76	95.83	138.25	180.16	194.54	208.38
$\pi/2$	0.1	58.47	78.29	108.44	125.87	144.43	148.57
$\pi/2$	0.2	42.92	56.34	75.04	84.98	95.88	96.35

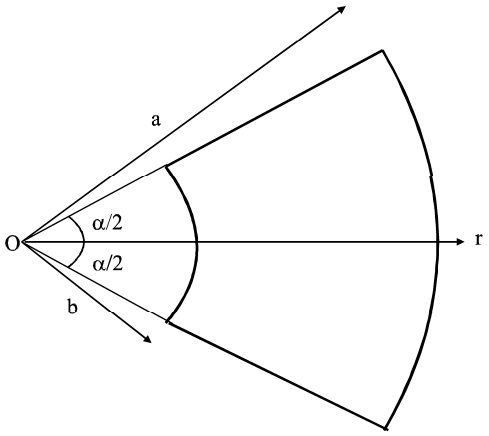

Figure 11. The annular sectoral plate

of circular plate with simply supports on Winkler foundation is considered for different foundation coefficients k. The total number of elements used are 288. 8 and 36 elements exist in radial and angular directions, respectively. To solve this kind of problem, term in Eq. (16) is added to the functional.

$$I = I_p + I_f,$$
$$I_f = \frac{1}{2}[k\mathrm{w}, \mathrm{w}]. \qquad (16)$$

This problem is solved and the effect of variation of k on the ($\bar{\omega}_{00}$) frequency parameter for Winkler foundation is shown in Fig. (13).

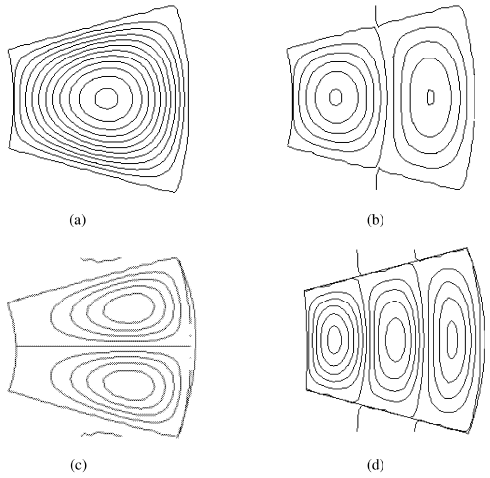

Figure 12. The counter lines of simply supported sectoral plate

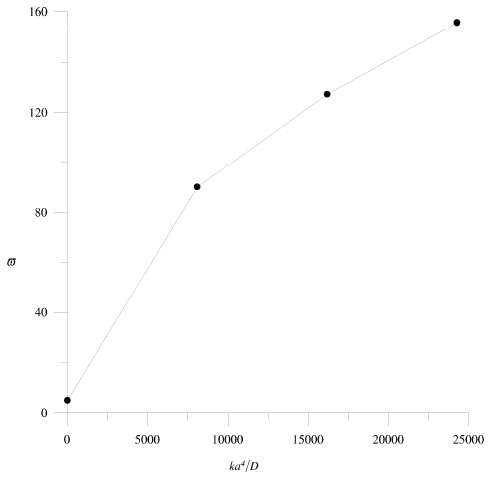

Figure 13. The effect of variation of k on the ω_{00} frequency parameter for Winkler foundation

6. Conclusion

In this paper, a free vibration analysis of circular, annular and annular sectoral plates based on Reissner theory has been presented. Two different elements (SEC24-SEC32) are used. The performance of the elements has also been investigated through the representative problems. From this study, it can be concluded that the values of the present analysis agree well with other solutions. For this study, the following remarks can be made:

1. The functional used in this study has only first order derivatives, therefore, bilinear shape functions are used and two elements (SEC24-SEC32) are obtained in an explicit form.

2. SEC24 and SEC32 avoid the shear locking and converge to the Kirchhoff solution for thin plates. Therefore, SEC24 and SEC32 based on Reissner plate theory are valid for analysis of thick as well as thin plates.

3. SEC24 and SEC32 provide accurate solution.

4. To assess the performance of SEC24 and SEC32, circular plates with several boundary conditions, annular plates and annular sectoral plates are solved. The frequency parameters of these plates are compared with theoretical results and good agreement is achieved.

5. The frequency parameters obtained by Reissner plate theory are lower than the ones given by Kirchhoff plate theory as expected.

6. The dynamic analysis of thick circular plates resting on Winkler foundation is performed and reasonable results are obtained.

References

[1] E. Reissner, J. Appl. Mech., ASME **12**, 69 (1946).
[2] E. Reissner, Int. J. Solids Structures **11**, 569 (1975).
[3] R. D. Mindlin, J. Appl. Mech., ASME **18**, 31 (1951).
[4] T. J. R. Hughes, R. L. Taylor, and W. Kanoknukkulchai, Int. J. Numer. Methods Eng. **11**, 1529 (1977).
[5] E. Hinton and N. Bicanic, Computers & Structures **10**, 483 (1979).
[6] O. C. Zienkiewicz, R. L Taylor, and J. Too, Int. J. Numerical Methods Eng. **3**, 275 (1971)
[7] J. L. Batoz and A. Lardeur, Int. J. Numer. Methods Eng. **28**, 533 (1989).
[8] T. Belytschko, C. S. Tsay, and W. K. Liu, Computer Methods in Applied Mechanics and Engineering **29**, 313 (1981).
[9] N. Eratlı and A. Y. Aköz, Computers & Structures **65**, 515 (1997).
[10] A. Y. Aköz and N. Eratlı, Structural Engineering and Mechanics **9**, 519 (2000).
[11] V. Panc, Theories of Elastic Plates, Noordhoff International Publishing (1975).
[12] J. D. Oden and J. N. Reddy, Variational method in theoretical mechanics (Springer, 1976).
[13] A. L. Goldenveizer, Theory of elastic thin shells (Pergomon Press, NewYork 1961).
[14] A. Y. Aköz and A. Özütok, Int. J. Numerical Methods in Engineering **47**, 1933 (2000).
[15] A. W. Leissa and Y. Narita, J. Sound and Vibration **70**, 221 (1980).
[16] A. W. Leissa, Vibration of plates, NASA SP 160, Washington, D.C.: U.S. Government Printing Office (1969).
[17] T. Irie, G. Yamada, and K. Takagi, J. Applied Mechanics, ASME **49**, 633 (1982).
[18] C. Liu and G. Chen, Int. J. Mech. Sci. **37**, 861 (1995).
[19] Y. Xiang, K. M. Liew, and S. Kitipornchai,

J. Engineering Mechanics, ASCE **119**, 1579 (1993).
[20] I. E. Harik and H. R. Molaghasemi, J. of Engineering Mechanics, ASCE **115**, 2709 (1989).
[21] T. Mizusawa, J. Sound and Vibration **149**, 461 (1991).
[22] T. Mizusawa, J. Sound and Vibration **150**, 245 (1991).

Appendix I

Notation

$M_r, M_\theta, M_{r\theta}$: bending moments
Q_r, Q_θ: shear forces
q: distributed load
k: spring coefficient of foundation
w: displacement of plate
Ω_r, Ω_θ : the components of the rotation of a normal to the middle plane of the plate, respectively
a : radius of plate
h : thickness of plate
E, ν, G, D : modules of elasticity, Poisson's ratio, shear modules of elasticity and plate rigidity, respectively
I (y) : functional
$<,>,[,]$: inner product
$[,]_\epsilon$: geometric (kinematic) boundary condition
$[,]_\sigma$: dynamic (natural) boundary condition
ψ_i : shape functions (i=1,...,3 for SEC24 or i=1,...,4 for SEC32)
s, η : non-dimensional coordinates of a master element
$[k]_{24}, [k]_{32}$: SEC24 and SEC32 finite element matrices
L : coefficient matrix
f : load vector
y : unknown vectors
$[\mathbf{K}], [\mathbf{M}], [\mathbf{K}^*]$: system matrix, mass matrix and condensed matrix vectors, respectively
[m] : mass matrix of element
$\rho, \bar{\rho}$: mass density per unit volume and per unit area, respectively
$\omega, \bar{\omega}$: natural angular frequency and frequency parameter, respectively.

Appendix II

For SEC24 element (Fig. 2),

$$\begin{aligned}\psi_1 &= (1-s),\\ \psi_2 &= s\,(1-\eta),\\ \psi_3 &= s\,\eta,\end{aligned} \tag{A.1}$$

where

$$\begin{aligned}s &= \frac{r}{r_2},\\ \eta &= \frac{\theta-\theta_1}{\triangle\theta}.\end{aligned} \tag{A.2}$$

For SEC32 element (Fig. 3),

$$\begin{aligned}\psi_1 &= (1-s)\,(1-\eta),\\ \psi_2 &= s\,(1-\eta),\\ \psi_3 &= s\,\eta,\\ \psi_4 &= (1-s)\,\eta,\end{aligned} \tag{A.3}$$

where

$$\begin{aligned}s &= \frac{r-r_1}{\Delta r},\\ \eta &= \frac{\theta-\theta_1}{\Delta\theta}.\end{aligned} \tag{A.4}$$

The element matrices $[k]_{24}, [k]_{32}$ for SEC24 and SEC32 are obtained as follows:

$$[k]_{24} = \begin{array}{c} \begin{array}{cccccccc} M_r & M_\theta & M_{r\theta} & Q_r & Q_\theta & \Omega_r & \Omega_\theta & w \end{array} \\ \begin{bmatrix} \gamma_1[K_1]_{24} & \gamma_2[K_1]_{24} & 0 & 0 & 0 & [K_2]_{24} & 0 & 0 \\ & \gamma_1[K_1]_{24} & 0 & 0 & 0 & [K_3]_{24} & [K_4]_{24} & 0 \\ & & \gamma_3[K_1]_{24} & 0 & 0 & [K_4]_{24} & [K_2-K_3]_{24} & 0 \\ & & & \gamma_4[K_1]_{24} & 0 & [K_1]_{24} & 0 & [K_2]_{24} \\ & & & & \gamma_4[K_1]_{24} & 0 & [K_1]_{24} & [K_4]_{24} \\ & & & & & 0 & 0 & 0 \\ & & & & & & 0 & 0 \\ & & & & & & & \gamma_5[K_1]_{24} \end{bmatrix} \end{array} \tag{A.5}$$

$$[k]_{32} = \begin{array}{c} \begin{array}{cccccccc} M_r & M_\theta & M_{r\theta} & Q_r & Q_\theta & \Omega_r & \Omega_\theta & w \end{array} \\ \begin{bmatrix} \gamma_1[K_1]_{32} & \gamma_2[K_1]_{32} & 0 & 0 & 0 & [K_2]_{32} & 0 & 0 \\ & \gamma_1[K_1]_{32} & 0 & 0 & 0 & [K_3]_{32} & [K_4]_{32} & 0 \\ & & \gamma_3[K_1]_{32} & 0 & 0 & [K_4]_{32} & [K_2-K_3]_{32} & 0 \\ & & & \gamma_4[K_1]_{32} & 0 & [K_1]_{32} & 0 & [K_2]_{32} \\ & & & & \gamma_4[K_1]_{32} & 0 & [K_1]_{32} & [K_4]_{32} \\ & & & & & 0 & 0 & 0 \\ & & & & & & 0 & 0 \\ & & & & & & & \gamma_5[K_1]_{32} \end{bmatrix} \end{array} \tag{A.6}$$

where

$$\gamma_1 = \frac{-12}{Eh^3},$$

$$\gamma_2 = \frac{-12\,\nu}{Eh^3},$$

$$\gamma_3 = \frac{-24\,(1+\nu)}{Eh^3},$$

$$\gamma_4 = \frac{-12\,(1+\nu)}{5Eh},$$

$$\gamma_5 = k. \tag{A.7}$$

The explicit form of the submatrices $[K_1]_{24}, [K_2]_{24}, [K_3]_{24}$, $[K_4]_{24}$, $[K_1]_{32}$, $[K_2]_{32}$, $[K_3]_{32}$, $[K_4]_{32}$ are given in Eq. (A.8-A.17). Submatrices for SEC24 element,

$$[K_1]_{24} = \int_0^{r_2}\int_{\theta_1}^{\theta_2} \psi_i\,\psi_j\,r\,dr\,d\theta = \begin{bmatrix} \frac{A_1B_1}{12} & \frac{A_1B_1}{24} & \frac{A_1B_1}{24} \\ \frac{A_1B_1}{24} & \frac{A_1B_1}{12} & \frac{A_1B_1}{24} \\ \frac{A_1B_1}{24} & \frac{A_1B_1}{24} & \frac{A_1B_1}{12} \end{bmatrix} \tag{A.8}$$

$$[K_2]_{24} = \int_0^{r_2}\int_{\theta_1}^{\theta_2} \psi_i\,\psi_{j\,,r}\,r\,dr\,d\theta = \begin{bmatrix} \frac{-B_2}{6} & \frac{B_2}{12} & \frac{B_2}{12} \\ \frac{-B_2}{6} & \frac{B_2}{9} & \frac{B_2}{18} \\ \frac{-B_2}{6} & \frac{B_2}{18} & \frac{B_2}{9} \end{bmatrix} \tag{A.9}$$

$$[K_3]_{24} = \int_0^{r_2}\int_{\theta_1}^{\theta_2} \psi_i\,\psi_j\,dr\,d\theta = \begin{bmatrix} \frac{B_2}{3} & \frac{B_2}{12} & \frac{B_2}{12} \\ \frac{B_2}{12} & \frac{B_2}{9} & \frac{B_2}{18} \\ \frac{B_2}{12} & \frac{B_2}{18} & \frac{B_2}{9} \end{bmatrix} \tag{A.10}$$

$$[K_4]_{24} = \int_0^{r_2}\int_{\theta_1}^{\theta_2} \psi_i\,\psi_{j\,,\theta}\,dr\,d\theta = \begin{bmatrix} 0 & \frac{-r_2}{6} & \frac{r_2}{6} \\ 0 & \frac{-r_2}{6} & \frac{r_2}{6} \\ 0 & \frac{-r_2}{6} & \frac{r_2}{6} \end{bmatrix} \tag{A.11}$$

where

$$A_1 = r_2^2,$$

$$B_1 = \theta_2 - \theta_1,$$

$$B_2 = r_2 B_1. \tag{A.12}$$

Submatrices for SEC32 element,

$$[K_1]_{32} = \int_{r_1}^{r_2}\int_{\theta_1}^{\theta_2} \psi_i\, \psi_j\, r\, dr\, d\theta = \begin{bmatrix} \frac{A_3A_4B_9}{36} & \frac{A_3A_6B_9}{36} & \frac{A_3A_6B_9}{72} & \frac{A_3A_4B_9}{72} \\ \frac{A_3A_6B_9}{36} & \frac{A_3A_5B_9}{36} & \frac{A_3A_5B_9}{72} & \frac{A_3A_6B_9}{72} \\ \frac{A_3A_6B_9}{72} & \frac{A_3A_5B_9}{72} & \frac{A_3A_5B_9}{36} & \frac{A_3A_6B_9}{36} \\ \frac{A_3A_4B_9}{72} & \frac{A_3A_6B_9}{72} & \frac{A_3A_6B_9}{36} & \frac{A_3A_4B_9}{36} \end{bmatrix} \tag{A.13}$$

$$[K_2]_{32} = \int_{r_1}^{r_2}\int_{\theta_1}^{\theta_2} \psi_i\, \psi_{j,r}\, r\, dr\, d\theta = \begin{bmatrix} \frac{A_1B_9}{18} & \frac{-A_1B_9}{18} & \frac{-A_1B_9}{36} & \frac{A_1B_9}{36} \\ \frac{A_2B_9}{18} & \frac{-A_2B_9}{18} & \frac{-A_2B_9}{36} & \frac{A_2B_9}{36} \\ \frac{A_2B_9}{36} & \frac{-A_2B_9}{36} & \frac{-A_2B_9}{18} & \frac{A_2B_9}{18} \\ \frac{A_1B_9}{36} & \frac{-A_1B_9}{36} & \frac{-A_1B_9}{18} & \frac{A_1B_9}{18} \end{bmatrix} \tag{A.14}$$

$$[K_3]_{32} = \int_{r_1}^{r_2}\int_{\theta_1}^{\theta_2} \psi_i\, \psi_j\, dr\, d\theta = \begin{bmatrix} \frac{A_8}{9} & \frac{A_8}{18} & \frac{A_8}{36} & \frac{A_8}{18} \\ \frac{A_8}{18} & \frac{A_8}{9} & \frac{A_8}{18} & \frac{A_8}{36} \\ \frac{A_8}{36} & \frac{A_8}{18} & \frac{A_8}{9} & \frac{A_8}{18} \\ \frac{A_8}{18} & \frac{A_8}{36} & \frac{A_8}{18} & \frac{A_8}{9} \end{bmatrix} \tag{A.15}$$

$$[K_4]_{32} = \int_{r_1}^{r_2}\int_{\theta_1}^{\theta_2} \psi_i\, \psi_{j,\theta}\, dr\, d\theta = \begin{bmatrix} \frac{A_3}{6} & \frac{A_3}{12} & \frac{-A_3}{12} & \frac{-A_3}{6} \\ \frac{A_3}{12} & \frac{A_3}{6} & \frac{-A_3}{6} & \frac{-A_3}{12} \\ \frac{A_3}{12} & \frac{A_3}{6} & \frac{-A_3}{6} & \frac{-A_3}{12} \\ \frac{A_3}{6} & \frac{A_3}{12} & \frac{-A_3}{12} & \frac{-A_3}{6} \end{bmatrix} \tag{A.16}$$

where

$$\begin{aligned} A_1 &= 2r_1 + r_2, \\ A_2 &= 2r_2 + r_1, \\ A_3 &= r_1 - r_2, \\ A_4 &= 3r_1 + r_2, \\ A_5 &= 3r_2 + r_1, \\ A_6 &= r_1 + r_2, \\ A_8 &= A_3B_9, \\ B_9 &= \theta_1 - \theta_2. \end{aligned} \tag{A.17}$$